

PRAMANA
— journal of
physics

© Indian Academy of Sciences

Vol. 77, No. 5
November 2011
pp. 843–853

Collective dynamics of multicellular systems

R MAITHREYE^{1,2}, C SUGUNA¹ and SOMDATTA SINHA^{1,*}

¹Centre for Cellular and Molecular Biology (CSIR), Uppal Road, Hyderabad 500 007, India

²Present address: Indian Institute of Technology-Madras, Chennai 600 036, India

*Corresponding author. E-mail: suguna@cmb.res.in; sinha@cmb.res.in

Abstract. We have studied the collective behaviour of a one-dimensional ring of cells for conditions when the individual uncoupled cells show stable, bistable and oscillatory dynamics. We show that the global dynamics of this model multicellular system depends on the system size, coupling strength and the intrinsic dynamics of the cells. The intrinsic variability in dynamics of the constituent cells are suppressed to stable dynamics, or modified to intermittency under different conditions. This simple model study reveals that cell–cell communication, system size and intrinsic cellular dynamics can lead to evolution of collective dynamics in structured multicellular biological systems that is significantly different from its constituent single-cell behaviour.

Keywords. Nonlinear regulation; bistable; oscillations; biochemical pathway; synchronization; multicell system.

PACS Nos 05.45.Xt; 87.18.–h

1. Introduction

Multicellular ensembles comprise groups of many cells either in a population or as structured ensembles of cells in tissues and organs. Generally, these systems are required to perform specialized functions. In an uncorrelated and independent cell population, the population behaviour is a simple sum of the individual cell behaviours. When cells in a population/tissue interact, the ensemble can show a unified collective behaviour, which is not just a ‘sum of the parts’, as the individual behaviour of the cells is regulated by the cell–cell interactions [1]. Cells in tissues and organs are examples where interactions can be directly through membrane-bound molecules, gap junctions, diffusion of secreted chemicals, etc. [2]. Cell-to-cell communication and signalling is essential for efficient functioning of the multicell systems. Emergence of the observed macroscopic behaviour depends on the type and strength of the interactions among the constituent cells and their local cellular behaviour. Cell-to-cell signalling by various means (e.g., diffusion of chemicals or sharing of membrane voltages) lead to different types of synchronized emergent dynamics, which, in some cases may be necessary for the normal function of the tissue or organism, but in others it may have pathological consequences. For example, in the

beta cells of the islets of Langerhans, synchronized bursting electrical activity precedes normal release of insulin, whereas in the case of epileptic seizures, synchronized activity in the cortical cells is pathological and occurs during the seizure [3,4]. Thus identifying conditions under which synchronized activity may emerge or not are important in health and disease.

Modelling studies have looked at different aspects of synchronization via coupling and given insight into these phenomena [5]. In biological systems, studies have shown traveling waves and other phenomena mediated by ions, such as calcium, in networks of cells connected via gap junctions [6]. At the individual cell level, a complex intracellular network of interacting biochemical pathways governs the functional behaviour of the cells. Thus, the collective behaviour of a cellular ensemble, in response to a variety of signals and perturbations, is a result of both intra- and intercellular processes that happen at different space and time-scales involving both short- and long-range feedback loops [7–9]. The most common form of regulation observed in intracellular pathways is the negative feedback [10,11]. Negative feedback is crucial in developmental programmes, which depend on the ability of cells to exhibit precise and reliable dynamical responses. Such processes are important in stabilizing the system to environmental perturbations, help in conserving energy and maintaining homeostasis in cellular processes [12–19].

In this paper, we have addressed the issue of evolution of collective behaviour in a structured population of model cells that incorporate a simple three-step negatively autoregulated biochemical pathway. The pathway is stable for basal parameter values, but loses stability through a sub-critical Hopf bifurcation on changes in parameters [16,18]. Thus, this pathway can exhibit stable, oscillatory and bistable (coexisting stable steady state and stable limit cycle) dynamics for different parameter regimes [15–18]. The model for the structured multicell system is considered to be a ring of cells, where each cell communicates with its two nearest neighbours through diffusion of the end product of the model cells that incorporate three-step pathway.

We have studied the collective behaviour of this one-dimensional lattice of the coupled cells with periodic boundary conditions for conditions when the individual cells would show stable, bistable and oscillatory dynamics. We have also studied the role of system size (cell number) and cell–cell communication strength (coupling strength) on the emergent dynamics of our model multicell system. We find that the global dynamics of the ring of cells can be similar or different from the local cellular dynamics depending on the ring size, coupling strength and the intrinsic dynamics of the cells. The intrinsic oscillations in cells are suppressed to stable dynamics, or modified to intermittency under different conditions. Thus this simple model study reveals that cell–cell communication, system size and intrinsic cellular dynamics can lead to the evolution of collective dynamics in structured multicellular biological systems that may be significantly different from the single-cell behaviour.

2. Model and methods

The single-cell and the corresponding multicell models are described in the following sections.

2.1 Single cell

Each model cell incorporates a simple three-step biochemical pathway regulated by end-product inhibition as shown in figure 1, where substrate A is converted to an end-product C, through the intermediate metabolite, B, and C inhibits the formation of A, by binding cooperatively to another molecule R to form a complex [CR]. The rate equations for the pathway reactions in the cell are described following the repressor-mediated inhibition process [17] as

$$\begin{aligned} \frac{dx}{dt} &= \left(\frac{\gamma}{1 + \gamma} \right) \frac{1}{1 + (1 + \gamma)z^n} - \alpha_1 x + \left(\frac{1}{1 + \gamma} \right), \\ \frac{dy}{dt} &= x - \alpha_2 y, \\ \frac{dz}{dt} &= y - \alpha_3 z - g. \end{aligned} \tag{1}$$

Here x , y and z represent the dimensionless concentrations of the reactants and the end-product A, B and C respectively. $\alpha_1, \alpha_2, \alpha_3$ are degradation rates of A, B and C; g is the utilization rate of the end-product C in cellular processes; γ is the strength of inhibition of A by the end-product through the cooperative binding of n molecules of C with R to form the [CR] complex, assuming a Michaelis–Menten-type of interaction.

The basal parameter values used in this study are $\gamma = 10, g = 4, n = 2, \alpha_1 = 1, \alpha_2 = 0.01, \alpha_3 = 0.01$ [17–19]. Earlier studies have shown that the pathway shows stable steady-state dynamics for basal parameter values, but more complex dynamics can be observed for other parameters [15–18].

2.2 Multicell system

The one-dimensional model multicellular system consists of a ring of these single cells coupled by diffusion of the end-product C between the neighbouring cells. The resultant

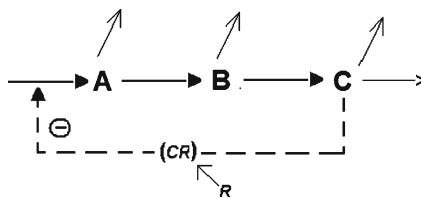


Figure 1. Three-step biochemical pathway with end-product inhibition mediated by the formation of a complex by the end-product with repressor, R . The arrows from the substrates A, B, C indicate degradation of the substrates and utilization of the end-product.

multicell system of N cells is modelled using a discretization scheme [20] and described by the following equations:

$$\begin{aligned} \frac{dx_i}{dt} &= \left(\frac{\gamma}{1+\gamma} \right) \frac{1}{1+(1+\gamma)z_i^n} - \alpha_1 x_i + \left(\frac{1}{1+\gamma} \right), \\ \frac{dy_i}{dt} &= x_i - \alpha_2 y_i, \\ \frac{dz_i}{dt} &= y_i - \alpha_3 z_i - g - e z_i + \frac{e}{2} (z_{i+1} + z_{i-1}). \end{aligned} \quad (2)$$

Here x_i , y_i and z_i are the concentrations of A, B and C in the i th cell, where i varies from 1 to N . The parameters g , n , α_1 , α_2 and α_3 are at their basal values in all the cells; e denotes the strength of coupling of z_i to the neighbouring cells, $i + 1$ and $i - 1$. For simulating this lattice system, periodic boundary conditions are used. We have studied the role of coupling e and lattice size N , for different values of feedback inhibition strength γ on the spatiotemporal dynamics of the multicell system by performing 50 simulations with randomly chosen initial conditions.

The temporal dynamics of the pathway is studied using XPPAUT [21]. Programmes for the lattice are written in FORTRAN 97 and MATLAB [22] is used for visualization.

2.3 Synchronization order parameter

The degree of synchronization is quantified using an order parameter, R , defined as the variance of the global signal to the spatial average of the variance of the local signal. It is given by

$$R = \frac{\langle [z_i]^2 \rangle - \langle [z_i] \rangle^2}{[\langle z_i^2 \rangle - \langle z_i \rangle^2]}, \quad (3)$$

where the symbols $\langle \ \rangle$ and $[\]$ represent the temporal and spatial averaging, respectively. R can take values between 0 (no synchronization) and 1 (completely synchronized).

3. Results and discussion

To study the role of system size, coupling strength and the local dynamics on the collective spatiotemporal global behaviour of the multicell system, we present our results in the following sections:

3.1 Single-cell behaviour

Figure 2 shows the temporal dynamics exhibited by a single cell incorporating a single pathway (figure 1). The pathway shows equilibrium dynamics for basal parameter values [15,16]. The bifurcation diagram in figure 2a shows that with increasing inhibition strength, γ , the equilibrium concentration of the end-product decreases rapidly till $\gamma \cong 35$, where it undergoes a subcritical Hopf bifurcation. Prior to this value of γ , the long-term dynamical behaviour is bistable, with the end-product concentration showing either

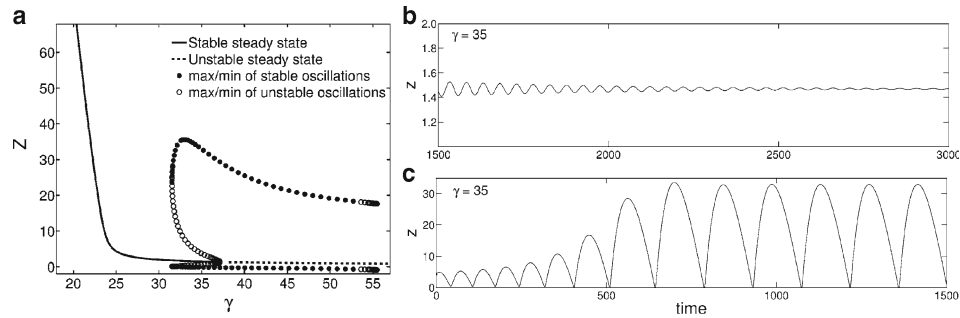


Figure 2. Dynamics of the end-product, z , of the pathway in a single cell for increasing γ , showing (a) Hopf bifurcation and bistable dynamics at $\gamma = 35$ for initial values of the end-product concentration, (b) $z_0 = 2.727$ and (c) $z_0 = 4.587$.

equilibrium (figure 2b) or stable limit cycle oscillations (figure 2c), for different initial values of A , B and C . These results indicate that in a clonal population of non-interacting cells (i.e., having this pathway with identical parameters), if the individual cells have unequal amounts of substrates due to stochasticity or any other reason, their local dynamics may be either oscillatory or stable dynamics.

3.2 Spatiotemporal dynamics of multicell system

When cells are coupled through diffusion of chemicals between their neighbours, the emergent collective behaviour can be the same or different from that of the constituent individual cells, for different coupling strengths and population sizes [6]. We present in the following sections, our study on the emergent behaviour of a ring of cells incorporating the above pathway and coupled through diffusion of z between the nearest neighbours (eq. (2)). For cells having pathways with $\gamma = 10$ (i.e., all exhibiting stable dynamics), the collective dynamics is also stable for all diffusive coupling e and population size N studied. We describe the spatiotemporal behaviour of the multicell system when individual cells are exhibiting bistable and oscillatory dynamics, for different e and N .

3.2.1 Local dynamics – Bistable. In the bistable region, each cell may show either equilibrium or oscillatory dynamics depending on the initial values of pathway variables. In table 1, we show the emergent dynamics at $\gamma = 35$, for the coupled multicell system comprising individual cells showing (i) all equilibrium, (ii) all oscillatory and (iii) a mix of stable and oscillatory dynamics, for different coupling strengths and lattice sizes.

For lattices comprising cells with equilibrium local dynamics, the global behaviour is stable for N and e studied for all 50 simulations. But, for oscillatory or mixed local dynamics, the global dynamics is stable for all lattice sizes for low coupling strengths ($e = 0.1$), and for large system sizes ($N = 50$) for increasing e . For $N = 10$ and 20 , global dynamics can be either oscillatory or stable for increasing coupling strength. Examples of these dynamic behaviours are shown in figure 3. Figure 3a shows the superposed time series of a mix of local stable and oscillatory dynamics with differing phases in the uncoupled cells.

Table 1. Global dynamics for different local dynamics.

Local dynamics of the cell	N	Global dynamics of the lattice		
		$e = 0.1$	$e = 0.3$	$e = 0.6$
Stable	10, 20, 50	Stable		
Oscillatory	10	Stable	74% stable 26% limit cycle	26% stable 74% limit cycle
	20, 50	Stable	Stable	Stable
Mixed	10	Stable	66% stable 34% limit cycle	36% stable 64% limit cycle
	20	Stable	Stable	88% stable 12% limit cycle
	50	Stable	Stable	Stable

Figure 3b shows the space–time plot of z where the stable and oscillatory local dynamics are colour-coded as in the colour bar, with cell number in horizontal and time in vertical directions. Figures 3c–f show the superposed time series and space–time plots of all cells for two representative lattices of 20 coupled cells where the emergent dynamics is synchronized either to equilibrium (figures 3c and d) or stable oscillations (figures 3e and f). Thus, the collective behaviour can be similar to the local dynamics of either type of cells (stable or oscillatory) in the bistable region. The results are the same for any ratio of stable and oscillatory cells.

3.2.2 Local dynamics – Oscillatory. At $\gamma = 45$, the pathway in single cells shows stable periodic oscillations for all initial conditions. We perform the same numerical simulations as is done in the earlier section with different coupling strengths and population sizes. The results are summarized for $e = 0.1, 0.3$ and 0.6 in table 2. There are two kinds of collective dynamical behaviour observed in the multicell systems – periodic and intermittent phase synchronization. The larger systems ($N = 50$) shows intermittent synchronization for all coupling strengths, but the smaller systems tend to synchronize to periodic dynamics, especially as coupling strength increases. We have checked the dynamics for longer time and for larger lattices and the cells continue to show intermittency with time and increasing lattice size.

Figure 4 shows the local and global dynamics for $N = 20$ cells for the coupling strength $e = 0.3$. Although all individual cells show the same oscillations in their local dynamics in z , when uncoupled (figures 4a, b), figures 4c–f show the global dynamics of the coupled cells, in two typical scenarios, where (i) all the cells are completely synchronized to oscillatory dynamics (figures 4c and d) and (ii) when they show intermittent phase synchronization (figures 4e and f).

To assess the extent of synchronization in these multicell systems of different sizes, we plot the parameter R (eq. (3)) for $N = 10, 20, 50$ and 100 for $0.1 < e < 0.9$ in figure 5. As described in table 2, the coupled multicell system shows varying levels of synchronization for different lattice sizes and coupling strengths. For example, for $N = 20$, the proportion

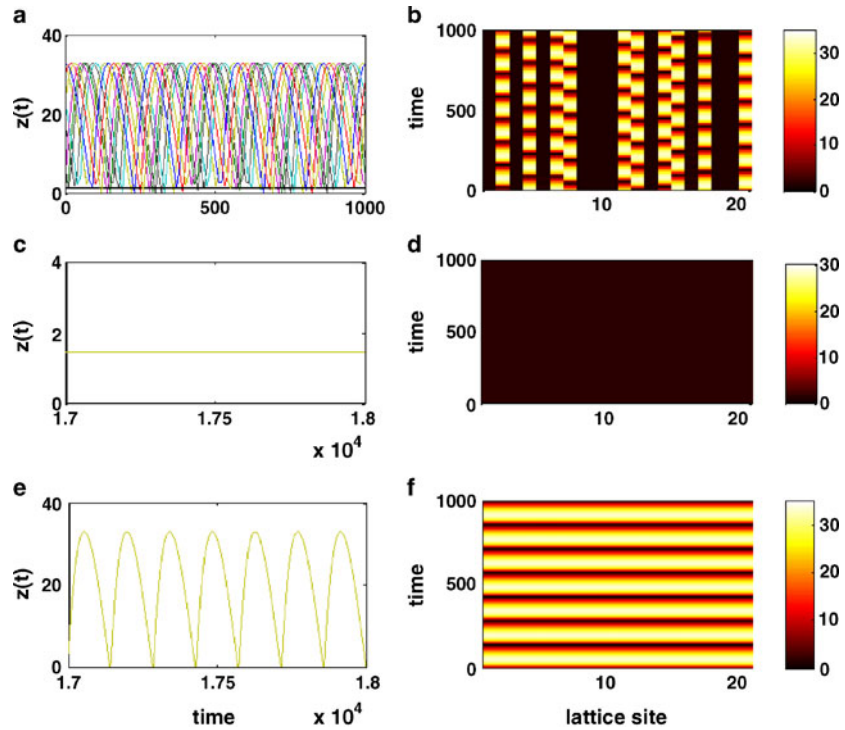


Figure 3. Dynamics of the end-product, z , for a mixed lattice of $N = 20$ cells with $\gamma = 35$ and diffusive coupling, $e = 0.6$, of the end-product, shown as time series (left column) and space–time plots (right column) for individual cells (**a**, **b**) and two coupled lattices synchronized to equilibrium (**c**, **d**) and oscillatory dynamics (**e**, **f**).

of lattices showing asynchrony (figures 4e and f) is larger for lower coupling strengths, and increased coupling induces all cells to oscillate in the same phase, thereby leading to complete synchronization ($R = 1$) in all lattices, as shown in figures 4c and d. This indicates that strong interactions between cells is necessary for synchronized collective behaviour and the local and global dynamics of cells in the multicell system are identical. However,

Table 2. Global dynamics for different system sizes (N).

N	Global dynamics of the lattice		
	$e = 0.1$	$e = 0.3$	$e = 0.6$
10	96% limit cycle 4% intermittent dynamics	All limit cycle	All limit cycle
20	Intermittent dynamics	96% limit cycle 4% intermittent dynamics	Limit cycle
50	Intermittent dynamics	Intermittent dynamics	Intermittent dynamics

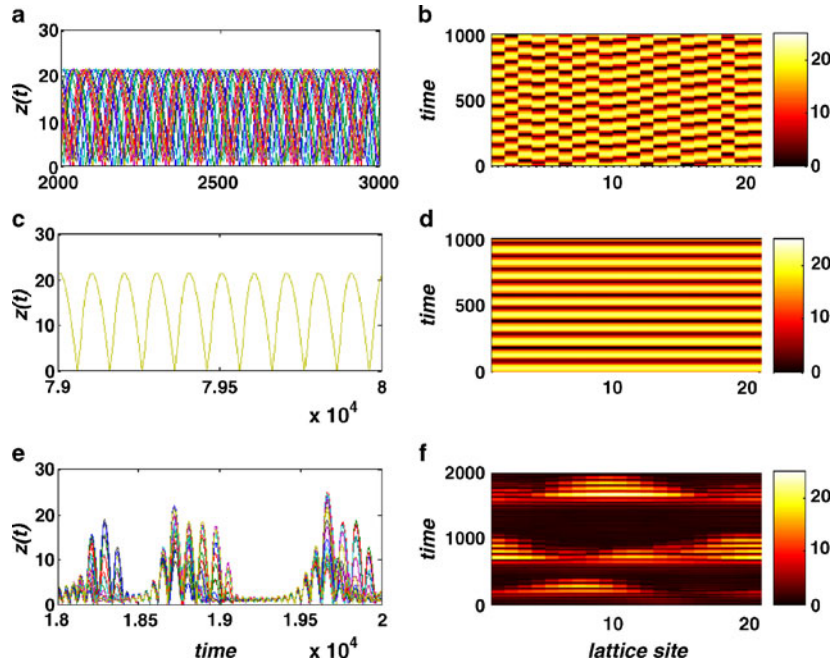


Figure 4. Dynamics of the end-product, z , for a ring of $N = 20$ cells with $\gamma = 45$ and $e = 0.3$, shown as time series (left column) and space–time plots (right column) for individual cells (a, b) and two coupled lattices showing complete synchronization to oscillations (c, d) and intermittent oscillations (e, f).

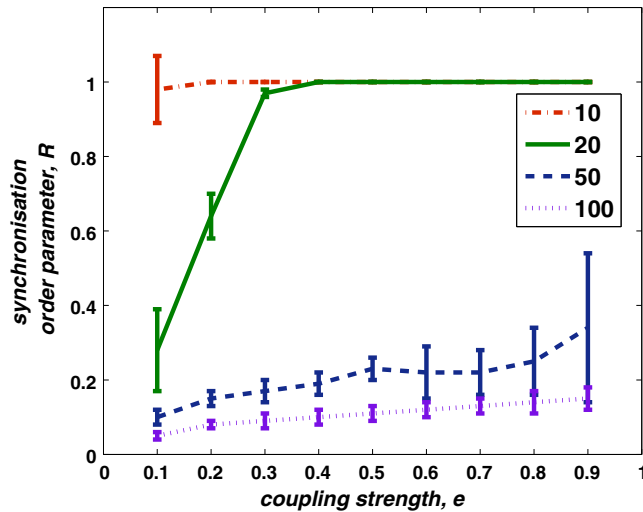


Figure 5. Synchronization order parameter for the end-product, z , for a ring of cells for varying N and e , for $\gamma = 45$.

for larger populations ($N = 50, 100$) there is very little effect of increased coupling on the ability of the cells to synchronize.

4. Conclusions

We have studied the role of cell–cell interaction strength, system size and the local cellular dynamics on the emergent dynamics of a model structured multicell system, with a view to understand how global behaviour may or may not reflect the intrinsic dynamics of the constituent cells. The single-cell dynamics is modelled based on the common motif of a simple three-step biochemical pathway with a single auto-inhibitory feedback loop. This pathway shows complex dynamics with a subcritical Hopf bifurcation, which allows stable, limit cycle and bistable (coexistence of stable steady state and stable oscillations) dynamics for changes in parameters. Subcritical bifurcations have been shown to result in hysteretic transitions between a stable steady state and stable large-amplitude oscillations [23], and also in membrane potential of neuronal cells as bursting oscillations [24], and in chemical systems such as, 1,4-cyclohexanedione-bromate reaction [25]. In this study, cell-to-cell coupling has been modelled through the diffusion of the end-product of the pathway. In biological systems, intercellular signalling commonly takes place through diffusion of the end-product of a pathway. Such interactions with other cells induce gene expression, differentiation and other collective activities, such as the quorum-sensing phenomenon [26,27].

When all the cells exhibit robust fixed point intrinsic dynamics at lower values of γ in figure 2, the collective dynamics in the ring of coupled cells is also stable for all couplings (e) and system sizes (N). Here the local and global dynamics are the same. But when the cells are oscillatory (at higher values of γ in figure 2), small lattices show synchronized oscillations, whereas large lattices show intermittent spatiotemporal dynamics irrespective of the strength of cell-to-cell coupling, as shown in figures 4e and f. Here the global dynamics of the ring of cells is the collective oscillations with varying amplitudes interspersed with transiently stable periods. This is quite different from the intrinsic regular oscillatory dynamics of the constituent cells. This result implies that the global dynamics can be different and of a new kind compared to the local cellular behaviour depending on the system size. When the cells are in the bistable region of γ , where cells can have a mix of intrinsic dynamics (stable and oscillatory) depending on intracellular concentrations of substrates, small rings of coupled cells show synchronized oscillations for increased strength of coupling, but large rings uniformly show stable dynamics, irrespective of the strength of coupling. This indicates that with varying constituent cell dynamics (a mix of stable or oscillatory), the global dynamics of multicell systems can be different depending on cell–cell interaction strength and system size.

That the emergent behaviour of cells in a multicell system can be quite different from the individual cell behaviour in isolation, has been found in the case of beta cells in the islet of Langerhans, where the isolated beta cells burst with a large range of frequencies with a fraction being silent, whereas they all burst synchronously with a medium frequency when they are coupled through gap junctions in the intact islets or in sufficiently large clusters [28]. Synchronized oscillations have been observed in many biological systems, such as glycolytic oscillations, vascular smooth muscles, cardiac and neuronal cells [29–38]. Such phenomena of change in global dynamics may also underlie developmentally regulated

tissue behaviour, where cell number, tissue size, and cell-cell communication may change with time.

Earlier theoretical work with activator–inhibitor-type of pathway [6] and ‘quorum-sensing’ type of circuits [26] have also shown emergent collective dynamics that remained similar to the intrinsic dynamics of the uncoupled cells or exhibited different types of synchronization. It has also been shown in the case of a multicellular system possessing birhythmicity, the collective behaviour, above a threshold number of cells, synchronize to only one type of oscillation irrespective of the inherent frequencies of individual cells, depending on the coupling strength [39]. Our results presented in this paper, thus, is not a property of the specific topology of the pathway chosen. Dynamic plasticity in constituent cells can get suppressed in larger systems, whereas smaller sized multicell systems can show either of the behaviour leading to phenotypic plasticity.

Acknowledgements

Authors thank the anonymous referee for critical comments, and the Department of Science and Technology, India for funding.

References

- [1] S Rajesh and Somdatta Sinha, *J. Biosci.* **33**, 289 (2008)
- [2] C Suguna and Somdatta Sinha, *Physica A* **346**, 154 (2005)
- [3] R Bertram and A Sherman, *J. Biosci.* **25**, 197 (2000)
- [4] D Somers and N Kopell, *Physica D* **89**, 169 (1995)
- [5] M Rosenblum, A Pikovsky and J Kurths, *Synchronisation, a universal concept in nonlinear sciences* (Cambridge University Press, Cambridge, UK, 2001)
- [6] S Rajesh, Sudeshna Sinha and Somdata Sinha, *Phys. Rev.* **E75**, 011906 (2007)
- [7] T Alarcon, H M Byrne and P K Maini, *SIAM J. Multiscale Model. Simul.* **3**, 440 (2005)
- [8] C S Nunemaker, R Bertram, A Sherman, K Tsaneva-Atanasova, C R Daniel and L S Satin, *Biophys. J.* **91**, 2082 (2006)
- [9] M Meyer-Hermann and R K P Benninger, *HFSP J.* **4**, 61 (2010)
- [10] E Selkov Jr, Y Grechkin, N Mikhailova and E Selkov, *Nucleic Acids Res.* **26**, 43 (1998)
- [11] D Thieffry, A M Huerta, E Perez-Rueda and J Collado-Vides, *Bioessays* **20**, 433 (1998)
- [12] A Becskei and L Serrano, *Nature* **405**, 590 (2000)
- [13] A Hoffmann, A Levchenko, M L Scott and D Baltimore, *Science* **298**, 1241 (2002)
- [14] T Gardner, C Cantor and J J Collins, *Nature* **403**, 339 (2000)
- [15] R Maithreye and Somdatta Sinha, *Modelling simple biochemical networks, in function and regulation of cellular systems: Experiments and Models* edited by A Deutsch, M Falcke, J Howard and W Zimmerman (Basle, Birkhauser, 2003)
- [16] R Maithreye and Somdatta Sinha, *Phys. Biol.* **4**, 48 (2007)
- [17] Somdatta Sinha and R Ramaswamy, *J. Theor. Biol.* **132**, 307 (1988)
- [18] Somdatta Sinha, *Biotech. Bioengg.* **31**, 117 (1988)
- [19] J J Tyson, *J. Theor. Biol.* **103**, 313 (1983)
- [20] Y Oono and S Puri, *Phys. Rev. Lett.* **58**, 836 (1987)
- [21] XPPAUT free software available at <http://www.math.pitt.edu/~bard/xpp/xpp.html>
- [22] MATLAB vendor web site <http://www.mathworks.com/products/matlab/>
- [23] J J Tyson, K C Chen and B Novak, *Curr. Opin. Cell Biol.* **15**, 221 (2003)
- [24] R Guttman, S Lewis and J Rinzel, *J. Physiol.* **305**, 377 (1980)

Collective dynamics of multicellular systems

- [25] B Zhao and J Wang, *J. Phys. Chem.* **A109**, 3647 (2005)
- [26] J Garcia-Ojalvo, M B Elowitz and S H Strogatz, *Proc. Natl. Acad. Sci.* **101**, 10955 (2004)
- [27] H Lodish, A Berk, S L Zipursky, P Matsudaira, D Baltimore and J Darnell, Cell-to-cell signaling: Hormones and receptors, in: *Molecular cell biology*, 4th edition (W H Freeman, New York, 2000)
- [28] P Smolen, J Rinzel and A Sherman, *Biophys. J.* **64**, 1668 (1993)
- [29] L Glass and M C Mackey, *From clocks to chaos. The rhythms of life.* (Princeton University Press, Princeton, NJ, 1988)
- [30] A Goldbeter, *Biochemical oscillations and cellular rhythms* (Cambridge University Press, Cambridge, UK, 1996)
- [31] A K Ghosh and B Chance, *Biochem. Biophys. Res. Commun.* **16**, 174 (1964)
- [32] J A Shapiro, *Annu. Rev. Microbiol.* **52**, 81 (1998)
- [33] M B Miller and B L Bassler, *Annu. Rev. Microbiol.* **55**, 165 (2001)
- [34] M Tsuchiya, S T Wong, Z X Yeo, A Colosimo, M C Palumbo, L Farina, M Crescenzi, A Mazzola, R Negri, M M Bianchi, K Selvarajoo, M Tomita and A Giuliani, *FEBS J.* **274**, 2878 (2007)
- [35] J Wolf and R Heinrich, *Biochem. J.* **345**, 321 (2000)
- [36] M Bier, B M Bakker and H V Westerho, *Biophys. J.* **78**, 1087 (2000)
- [37] S H Strogatz, *Nature (London)* **410**, 268 (2001)
- [38] M Rosenblum and A Pikovsky, *Contemp. Phys.* **44**, 401 (2003)
- [39] C Suguna and Somdatta Sinha, *Pramana – J. Phys.* **71**, 423 (2008)